Supporting Information: Structural Origins of Misfolding Propensity in the Platelet Adhesive Von Willebrand Factor A1 Domain

Michael T. Zimmermann[1], Alexander Tischer[2], Steven T. Whitten[3] and Matthew Auton[2*].

June 30, 2015

[1] Division of Biomedical Statistics and Informatics, Department of Health Sciences Research, Mayo Clinic, Rochester, MN

[2] Division of Hematology, Department of Internal Medicine, Mayo Clinic, Rochester, MN

[3] Department of Chemistry and Biochemistry, Texas State University, San Marcos, TX

[*] To whom correspondence is addressed, auton.matthew@mayo.edu.

Running Title: A Localized Thermodynamic Potential for VWF Platelet Adhesion.

1 Computational Controls

1.1 Spatial parsing of the m-value using SEED

To assess whether these residue specific thermodynamic contributions could be recapitulated in the context of fragments which are discontiguous along the proteins linear sequence, fragments were also generated by spatial proximity in the 3D structure. Spatial parsing was performed by progressively growing fragments according to next nearest residues determined from an alpha carbon distance difference matrix (Figure 3A&B). This enumeration produces $\sim N^2$ unique fragments of the domain structures; ∼36100 for A1 and ∼34969 for A3, but ∼8% of the total number of distinct enumerations generated by sequential and spatial parsing are shared in common. Within this spatial context, median m/F values of excised and in-situ fragments and cooperativity ratios were calculated and compared for both A1 and A3 domains (Figure 3C). This procedure generates a divergent ΔCR profile compared to the contiguous sequential parsing. Spatial parsing does not highlight concerted structural regions, but rather shows differences for residues scattered throughout the structure as sequentially discontiguous segments that are thermodynamically indistinguishable.

1.2 Differences in solvent accessible surface area alone is nondistinguishing

Fragment m-values are proportional to the summed group transfer free energies scaled by changes in solvent accessible surface area. In order to assess surface area contributions alone, the group transfer free energy terms were omitted from SEED's sequential parsing. The ΔASA of both excised and in-situ fragments of A1 are slightly greater than for A3, but the ratio $\Delta ASA_{excised}/\Delta ASA_{in\text{-}situ}$ of the domains are similar, yielding minimal differences in overall per-residue areas of the domains (Figure 4). Considering only ΔASA in the spatial parsing also does not identify A1 regions that are thermodynamically distinct from the corresponding A3 regions.

1.3 Cooperativity ratios are qualitatively independent of denaturant and osmolyte specific group transfer free energies

The computational dependence of SEED on group transfer free energies for different denaturants (GndHCl and Urea) and the protecting osmolytes (TMAO, Sarcosine, Sorbitol, Sucrose and Proline) was also assessed. Amino acid sidechain and backbone unit transfer free energies corresponding to urea and osmolytes were obtained from Auton & Bolen [1–3]. Transfer free energies to GndHCl were compiled from Nozaki & Tanford [4] and Sarker & Bolen [5]. Comparison of the sequential cooperativity ratios obtained for both denaturants and osmolytes shown in Figure S3A&B illustrates a qualitatively similar pattern, although not quantitatively identical. Differences in denaturant and osmolyte dependent group transfer free energies should result in quantitative differences, but, because SEED is a ratio-metric comparison between m-values of excised fragments relative to in-situ fragments, cooperativity ratios of both A1 and A3 have qualitatively similar trends. These results demonstrate that a specific thermodynamic property of the A1 domain structure is recognized by group transfer free energies that is discernibly different from that of the A3 domain structure.

2 Figure Legends

Figure 1: Sequence alignment implicated by the CE-based structure superpositioning and manual review of the residue equivalence.

Figure 2: Spatial parsing by SEED. A) Examples of excised and in-situ fragments derived from sequentially discontiguous regions of structure parsed through 3-dimensional space. Fragments are generated relative to a "root" residue i (red) extending through space by next nearest neighbor residues indicated in blue (two examples for each of two "roots" shown) until the structure is fully recapitulated. B) The same concept is shown in greater detail, beginning from the matrix of all pairwise alpha carbon distances. m-values are calculated for both excised and in-situ fragments, normalized to the number of residues in the fragments (m/F), and the median (horizontal lines) is calculated with respect to all fragment sizes with a common root residue, i. Median cooperativity ratio CR=($m_{excised}/m_{in\text{-}situ}$). C) Median per-residue m/F for excised and in-situ fragments (left), CR (middle), ΔCR (right).

Figure 3: Sequential parsing of the solvent accessible surface area by SEED. Median contribution of each residue to solvent accessible surface area changes upon unfolding by sequential parsing. A) Median per-residue fragment length normalized ΔASA/F is compared between A1 and A3 in excised and in-situ fragments. B) The median ΔASA Ratio, $\Delta ASA_{excised}/\Delta ASA_{in\text{-}situ}$, for the two domains. C) The difference in median ΔASA Ratio (A1 - A3) reveals little difference in per residue contributions to the total change in solvent accessible surface area upon unfolding. Note that the y-axis scale in panels B and C are identical to those in Figure 4 of the main manuscript.

Figure 4: Cooperativity ratio is qualitatively independent of denaturant and osmolyte type. Sequential parsing comparison of the A1 domain (A) and the A3 domain (B).

References

[1] Auton, M., L.M. Holthauzen & D.W. Bolen (2007) Anatomy of energetic changes accompanying urea-induced protein denaturation. PNAS 104:15317-15322.

[2] Auton, M. & D.W. Bolen (2005) Predicting the energetics of osmolyte-induced protein folding/unfolding. PNAS 102:15065-15068.

[3] Auton, M., & D.W. Bolen (2004) Additive transfer free energies of the peptide backbone unit that are independent of the model compound and the choice of concentration scale. Biochemistry 43:1329-1342.

[4] Nozaki, Y. & C. Tanford (1970) The solubility of amino acids, diglycine, and triglycine in aqueous guanidine hydrochloride solutions. J Biol Chem 245:1648-1652.

[5] Sarker, S. & D.W. Bolen (1993) Temperature Dependence of Solubility of Amino Acids and Model Peptides in Water and Different Concentrations of Guanidine Hydrochloride. Master's Thesis (Southern Illinois University at Carbondale, Carbondale, Illinois).

[6] Auton, M., J. Rösgen, M. Sinev, L.M. Holthauzen & D.W. Bolen (2011) Osmolyte effects on protein stability and solubility: A balancing act between backbone and side-chains. Biophys Chem 159:90-99.

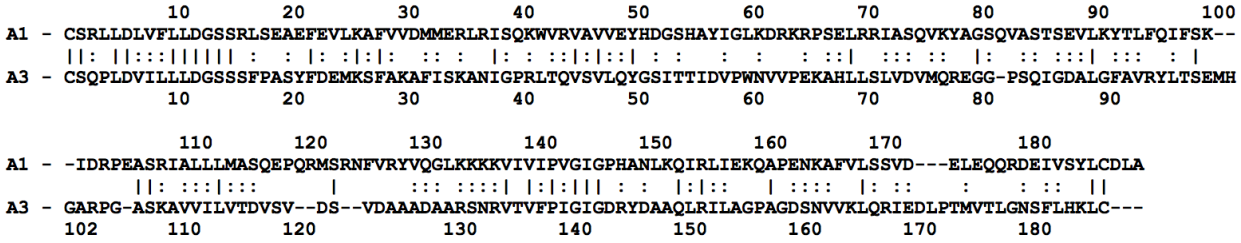

Figure 1: Sequence alignment implicated by the CE-based structure superpositioning and manual review of the residue equivalence.

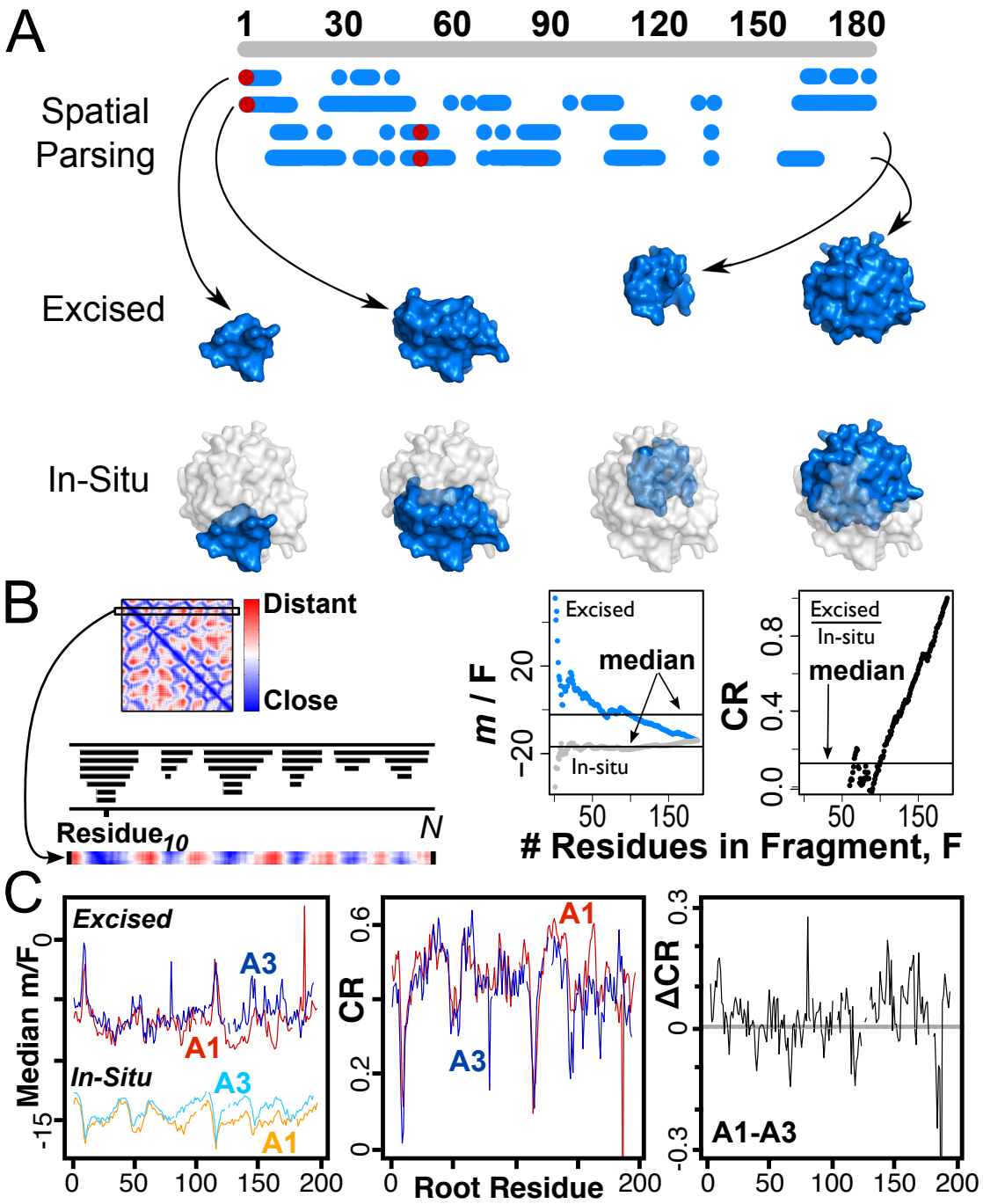

Figure 2: Spatial parsing by SEED. A) Examples of excised and in-situ fragments derived from sequentially discontiguous regions of structure parsed through 3-dimensional space. Fragments are generated relative to a "root" residue i (red) extending through space by next nearest neighbor residues indicated in blue (two examples for each of two "roots" shown) until the structure is fully recapitulated. B) The same concept is shown in greater detail, beginning from the matrix of all pairwise alpha carbon distances. m-values are calculated for both excised and in-situ fragments, normalized to the number of residues in the fragments (m/F), and the median (horizontal lines) is calculated with respect to all fragment sizes with a common root residue, i. Median cooperativity ratio CR=($m_{excised}/m_{in\text{-}situ}$). C) Median per-residue m/F for excised and in-situ fragments (left), CR (middle), ΔCR (right).

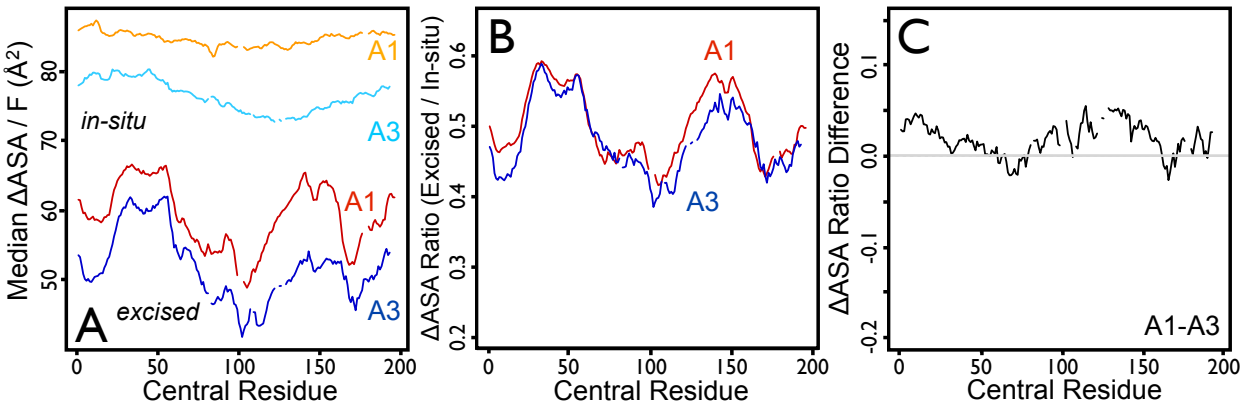

Figure 3: Sequential parsing of the solvent accessible surface area by SEED. Median contribution of each residue to solvent accessible surface area changes upon unfolding by sequential parsing. A) Median per-residue fragment length normalized ΔASA/F is compared between A1 and A3 in excised and in-situ fragments. B) The median ΔASA Ratio, $\Delta ASA_{excised}/\Delta ASA_{in\text{-}situ}$, for the two domains. C) The difference in median ΔASA Ratio (A1 - A3) reveals little difference in per residue contributions to the total change in solvent accessible surface area upon unfolding. Note that the y-axis scale in panels B and C are identical to those in Figure 4 of the main manuscript.

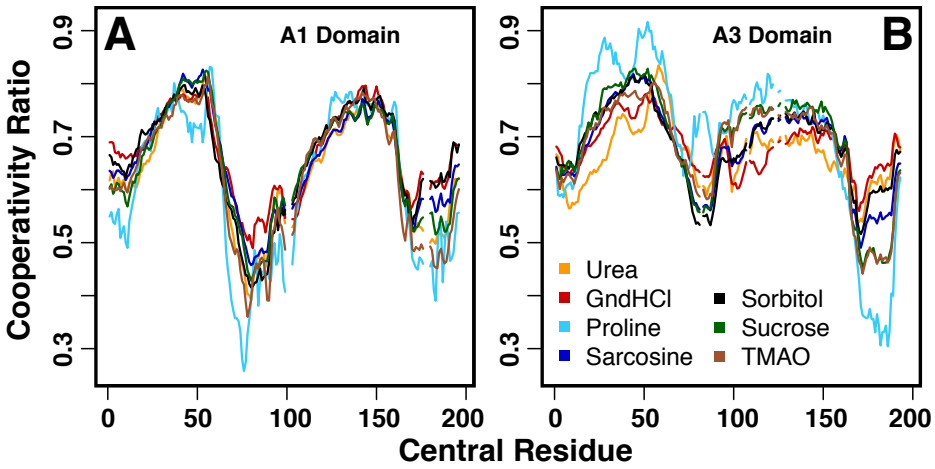

Figure 4: Cooperativity ratio is qualitatively independent of denaturant and osmolyte type. Sequential parsing comparison of the A1 domain (A) and the A3 domain (B).